Classification: Biological Sciences, Developmental Biology

Title: Divergence of gene regulatory network linkages during specification of ectoderm and mesoderm in early development of sea urchins

Short Title: Divergence of GRNs in early echinoid embryos

Author Affiliations:

Eric M. Erkenbrack[a,1,3] and Eric H. Davidson[a,2]

[a]Division of Biology and Biological Engineering, California Institute of Technology, Pasadena, California, 91125, United States of America

[1]Current address: Department of Ecology and Evolutionary Biology, Yale University, New Haven, Connecticut, 06511, United States of America

[2]Deceased author

[3]Corresponding Author

Eric M. Erkenbrack, Yale University, Department of Ecology and Evolutionary Biology, New Haven, CT, 06511, 203-737-3092, email: erkenbra@caltech.edu (EME), eric.erkenbrack@yale.edu (EME)

Keywords: gene regulatory network evolution, network topology, sea urchin embryogenesis, embryonic axis specification, cidaroid, euechinoid

Abstract

Developmental gene regulatory networks (GRNs) are assemblages of gene regulatory interactions that direct ontogeny of animal body plans. Studies of GRNs operating in early development of euechinoid sea urchins has revealed that little appreciable change has occurred since their divergence approximately 90 million years ago (mya). These observations suggest that strong conservation of GRN architecture has been maintained in early development of the sea urchin lineage. To test whether this is true for all sea urchins, comparative analyses of echinoid taxa that diverged deeper in geological time must be conducted. Recent studies highlighted extensive divergence of skeletogenic mesoderm specification in the sister clade of euechinoids, the cidaroids, suggesting that comparative analyses of cidaroid GRN architecture may confer a greater understanding of the evolutionary dynamics of developmental GRNs. Here, we report spatiotemporal patterning of 55 regulatory genes and perturbation analyses of key regulatory genes involved in euechinoid oral-aboral patterning of non-skeletogenic mesodermal and ectodermal domains in early development of the cidaroid *Eucidaris tribuloides*. Our results indicate that developmental GRNs directing mesodermal and ectodermal specification have undergone marked alterations since the divergence of cidaroids and euechinoids. Notably, statistical and clustering analyses of echinoid temporal gene expression datasets indicate that regulation of mesodermal genes has diverged more markedly than regulation of ectodermal genes. Although research on indirect-developing euechinoid sea urchins suggests strong conservation of GRN circuitry during early embryogenesis, this study indicates that since the divergence of cidaroids and euechinoids developmental GRNs have undergone significant divergence.

Significance Statement

Sea urchins consist of two subclasses, cidaroid and euechinoids. Research on gene regulatory networks (GRNs) in early development of three euechinoids indicates that little appreciable change has occurred to their linkages since they diverged approximately 90 million years ago (mya). We asked if this conservation extends to the all echinoids. Here we demonstrate extensive divergence of GRN architecture in early embryonic specification of the oral-aboral axis in echinoids. We systematically analyzed in a cidaroid spatiotemporal expression and function of regulatory genes segregating euechinoid ectoderm and mesoderm. While we found evidence for diverged regulation of both mesodermal and ectodermal genes, our comparative analyses indicated that, since these two clades diverged 268.8 million years ago, mesodermal GRNs have undergone significantly more alteration than ectodermal GRNs.

\body

Introduction

Integral to early development of a bilaterian is the development of the three embryonic tissue-layer domains: endoderm, ectoderm, and mesoderm. Asymmetrically distributed RNA and proteins in the egg provide the initial inputs into this process and thereby determine the spatial coordinates of domain formation (1, 2). In the context of these maternal factors, zygotic transcription of distinct sets of regulatory genes occurs in specific regions of the embryo, initiating the genomically encoded regulatory program and its output of regulatory genes. In this way the embryo becomes populated by distinct sets of transcription factors and cell signaling transcripts called regulatory states (3). The spatial readout of developmental gene regulatory networks (GRNs), regulatory states provide each cell with its molecularly distinct and functional identity (4, 5).

Sea urchins (class Echinodea) have long served as model systems to study mechanisms of early development and, more recently, to study fundamental aspects of developmental GRNs.

68 Diversification of cell lineages and embryonic domains in sea urchin embryos depends on the
69 cleavage positions of their blastomeres (6, 7), facilitating interpretation of mechanisms of spatial
70 change. Sea urchin lineages have undergone multiple changes in life history strategies, providing
71 a convenient framework, with experimental replicates, to investigate evolution and mechanisms of
72 developmental programs (8). Importantly, a well-represented fossil record affords dating of
73 evolutionary events (9) and has established that the sister subclasses of sea urchins—cidaroids
74 and euechinoids—diverged from one another at least 268.8 million years ago (mya) (10).
75 Differences in the timing of developmental events in embryogenesis of cidaroids and euechinoids
76 have long been a topic of interest, but only recently have become the subject of molecular
77 research (11-18).

78 Research on early development of the euechinoid purple sea urchin *Strongylocentrotus*
79 *purpuratus* has brought into high resolution the players and molecular logic directing
80 developmental GRNs that specify its varied embryonic domains and subdomains (19-30).
81 Additionally, abundant comparative evidence exists for other euechinoid taxa, including *Lytechinus*
82 *variegatus* (31-37) and *Paracentrotus lividus* (38-42). Data from these three indirect-developing
83 euechinoids indicate that, although these taxa diverged from one another approximately 90 mya
84 (9, 43), very little appreciable change to developmental GRNs has been observed in their early
85 development (44-46). While there is evidence of a few heterochronic alterations to these GRNs,
86 e.g. a heterochronic shift in *snail* expression in *L. variegatus* versus *S. purpuratus* (22), numerous
87 studies have made clear the striking conservation of GRN linkages and spatiotemporal gene
88 expression in these lineages. Recently, studies of early development of the distantly-related,
89 indirect-developing cidaroid sea urchin *Eucidaris tribuloides* revealed that skeletogenic mesoderm
90 specification in this clade is markedly different from that observed in euechinoids (17, 18, 47).
91 These observations suggest that comparative analyses of GRN circuitry in early development of

92 cidaroids and euechinoids have the potential to illuminate the tempo and mode of evolution of
93 developmental GRNs.

94 Here, we coupled comparative spatiotemporal gene expression analyses with experimental
95 manipulations of regulatory genes specifying euechinoid non-skeletogenic mesodermal (NSM) and
96 ectodermal domains in the cidaroid *E. tribuloides* to reveal how these GRNs have changed since
97 the divergence of these two clades 268.8 mya. This study focused on oral-aboral (O-A; also called
98 dorsal-ventral) patterning, which has consequences for both ectoderm and mesoderm. O-A axis
99 specification is a well-documented process in euechinoids (46) and is a highly conserved
100 developmental mechanism in deuterostomes (48, 49). We present evidence that deployment and
101 regulatory interactions of regulatory genes specifying sea urchin ectoderm and mesoderm have
102 diverged substantially in indirect-developing echinoids. Importantly, our comparative data and
103 analyses suggest that regulatory interactions occurring in ectodermal GRNs have undergone less
104 divergence than those occurring in mesodermal domains. Our conclusions are supported by
105 comparative spatiotemporal data, statistical analyses of timecourse gene expression data in three
106 taxa of echinoids and perturbation analyses. Taken together regulatory genes expressed in
107 ectodermal domains exhibited stronger signals of conservation relative to those expressed in
108 mesodermal domains. These results suggest that embryonic domains and cell types in early
109 development of sea urchins have evolved at different rates since the divergence of the two sister
110 sub-classes of modern sea urchins. These alterations to GRN architecture have occured
111 throughout the network and frequently since their divergence. Additionally, these results offer an in
112 principle explanation for observations of rapid change to nearly all components of developmental
113 process in the development of direct-developing, non-feeding sea urchins (50-53).
114

115 # Results

Ectodermal O-A regulatory states in the cidaroid *E. tribuloides* suggest striking conservation of regulatory gene deployment in echinoids

In euechinoids, ectoderm is segregated into a diverse set of regulatory states defined by the future location of the stomodeum (46, 54, 55). A critical factor in establishing oral-aboral (47) polarity in sea urchins is the signaling ligand *nodal* (35, 38). Nodal ligand activates the SMAD signaling pathway, which is directly upstream of *nodal* (itself), *not, lefty* and *chordin* in oral ectoderm (OE) (40, 56). In *E. tribuloides,* zygotic transcription of *nodal, not* and *lefty* begins by early blastula stage (Fig. 1*D*, 1*J*, and Fig. S1*D*). In contrast, transcriptional activation of *chordin* is delayed by at least 5 hours from this initial cohort, indicative of an intermediate regulator between *nodal* and *chordin* in *E. tribuloides* (Fig. 1D and 1E). From 17 hpf to 40 hpf, spatial expression of *nodal* is observed in a well-defined region in OE that expands slightly as gastrulation proceeds (Fig. 1D2-1D5 and Fig. S2). Unlike *nodal*, the spatial distribution of its targets is not solely restricted to a small field of cells in OE. *Lefty* (also known as Antivin), an antagonist of *nodal*, exhibits a broader pattern of expression that, by 50 hpf, expands into the oral side of the archenteron (Fig. S1D2-S1D5 and Fig. S2). Similarly, *chordin* transcripts are detected in OE throughout early *E. tribuloides* development (Fig. 1E1-1E5 and Fig. S2). The homeobox gene *not,* known to play a role directly downstream of *nodal* in euechinoid O-A ectodermal and mesodermal polarization (27, 57), was observed spatially in OE during gastrulation and later extends vegetally towards the perianal ectoderm and is observed in the archenteron (Fig. 1J1-1J5 and Fig. S2). In euechinoids, the *bmp2/4* ligand is a directly downstream of Nodal and is translocated across the embryo to the aboral side, where it stimulates via SMAD signaling in aboral ectoderm (AE) specification genes such as *tbx2/3* (38, 58, 59). In *E. tribuloides*, both *bmp2/4* and *tbx2/3* are

139 upregulated with the *nodal-not-lefty* cohort (Fig. S1G and Fig. 1I1-1I5). *Tbx2/3* exhibits spatial
140 expression from late blastula stage onwards that is complementary to OE genes in the lateral AE
141 (Fig. 1I2-1I5). By mid-gastrula stage, *tbx2/3* is also expressed in the archenteron and much later,
142 by 70 hpf, is expressed in the bilateral clusters of cells synthesizing the larval skeleton (Fig. S2),
143 which is similar to the spatial expression in two euechinoids with notably interesting heterochronic
144 differences (60, 61). Lastly, the Forkhead family transcription factor *foxq2* is sequentially restricted
145 to and specifically expressed in embryonic anterior neural ectoderm (ANE) territory in
146 deuterostomes (62). In euechinoids, *foxq2* restriction to ANE is a crucial component of O-A axis
147 specification, setting the anterior boundary of OE by restricting expression of *nodal* (23, 55). In *E.*
148 *tribuloides, foxq2* exhibited an expression pattern consistent with observations in euechinoids and
149 other deuterostomes, suggesting conserved roles for this gene in ANE and O-A specification (Fig.
150 1B and Fig. S2).

151 Conserved spatiotemporal deployment of ciliary band regulatory 152 genes

153 Free-feeding, indirect-developing sea urchins possess a single neurogenic ciliated band
154 (CB) early in development that circumnavigates the larval oral face and facilitates feeding and
155 locomotion (63). This structure has undergone frequent modification in the lineages leading to
156 modern sea urchins, viz. in planktotrophic larvae (64). In euechinoids *goosecoid (gsc), onecut* and
157 *irxa* contribute to the geometric patterning of CB formation (28, 40, 65). In euechinoids, *gsc* is
158 expressed in OE and is directly downstream of *nodal* signaling on the oral side of the embryo (40);
159 *onecut* (also known as *hnf6*) is a ubiquitous, maternally deposited factor that is restricted to a
160 region spanning the boundaries of OE and AE, at which lies progenitor CB territory; and *irxa* is
161 expressed exclusively in AE downstream of *tbx2/3* (40, 66). In the cidaroid *E. tribuloides*, *gsc* is

162 activated with the OE cohort and is also spatially restricted to OE (Fig. 1G1 and Fig. S3). As in
163 euechinoids, *onecut* is maternally deposited in *E. tribuloides* (Fig. 1H1). Although its early spatial
164 expression was not obtained, staining was observed in a restricted band of cells encircling the OE
165 by mid-gastrula stage. The spatial dynamics of *onecut* in *E. tribuloides* is notable insofar as its
166 spatial distribution in progenitor CB begins in the progenitor field of post oral CB and subsequently
167 extends in a narrow band of 4-8 cell diameters towards progenitor pre oral CB (Fig. 1H2-1H5 and
168 Fig. S3). This observation starkly contrasts that in euechinoids, in which *onecut* is observed
169 ubiquitously expressed early and later delimited as a whole to the CB territory by transcriptional
170 repressors in the OE and AE (28, 67). *Irxa* initiates zygotic expression at mid-blastula stage (~14
171 hpf) in *E. tribuloides*, and by 28 hpf is observed broadly in AE (Fig. 1C1-1C5). Unlike in
172 euechinoids, *irxa* is broadly distributed in *E. tribuloides* AE—much more so than *tbx2/3*—indicating
173 that it is likely broadly activated in the ectoderm and repressed in OE and ANE. These
174 spatiotemporal observations of key CB regulatory genes suggest that CB patterning mechanisms
175 are likely to be conserved in echinoids.

176 Non-skeletogenic mesodermal patterning and regulatory interactions 177 have diverged widely in echinoids

178 Non-skeletogenic mesoderm (NSM) in euechinoids arises at the vegetal plate from early
179 cleavage endomesodermal precursors and gives rise to four different cell types: blastocoelar cells,
180 pigment cells, circumesophageal cells and coelomic pouch cells (68). Experimental observations
181 indicate that euechinoids completely rely on presentation of Delta ligand in the adjacent SM to
182 upregulate NSM regulatory factors in veg2 endomesodermal cells (32, 69, 70). After Delta/Notch
183 signaling upregulates NSM regulatory genes in SM-adjacent cells, NSM is partitioned into aboral
184 NSM and oral NSM as a result of Nodal/SMAD signaling upregulating transcription factor *not* on

185 the oral side of the embryo (27, 71). The first evidence of NSM polarity in *E. tribuloides*, is seen in
186 the spatial distribution of *ese* and *gcm* transcripts shortly after gastrulation has commenced (Fig.
187 1K2-1K5 and 1L2-1L5). In euechinoids, *ese* is expressed in the oral NSM, and *gcm* is expressed in
188 the aboral NSM. In *E. tribuloides ese* is first in ANE and progenitor NSM just prior to the onset of
189 gastrulation, shortly after invagination of the archenteron it is subsequently restricted to one side in
190 NSM (Fig. 1K2-1K5). Similarly, *gcm* is expressed transiently in oral and aboral NSM, and by 28 hpf
191 is restricted to a cluster of cells just below the tip of the archenteron (Fig. 1L2-1L5). Later this
192 expression is seen solely on one side of the archenteron as *gcm*-positive cells ingress rapidly into
193 the blastocoel at 36 hpf (Fig. S4). Double fluorescent whole-mount *in situ* hybridization (WMISH)
194 revealed that *ese* and *gcm* in this cidaroid are restricted to opposite sides of the archenteron (Fig
195 S4G1 and S4G2), providing the first evidence of conserved polarity in NSM segregation in
196 echinoids.

197 To further clarify NSM regulatory states in *E. tribuloides* and their similarity to those in
198 euechinoids, we conducted additional single and double WMISH on NSM regulatory genes *ets1/2,*
199 *gatac, gatae, prox, scl* and *tbrain.* Directly downstream of *gcm* in euechinoids is *gatae* (27). In *S.*
200 *purpuratus*, *gatae* is observed in endomesoderm by blastula stage (72). In *E. tribuloides* NSM,
201 *gatae* is expressed throughout the endomesoderm at the time of SM ingression (~28 hpf) and later
202 is observed restricted to one side near the tip of the archenteron, as well as in the second wave of
203 ingressing mesenchyme (Fig. S1C2-S1C5 and Fig. S4). *Gatac (gata1/2/3), prox* and *scl*, all of
204 which are oral NSM genes in euechinoids (27), come off the baseline at similar times in *E.*
205 *tribuloides* and are detectable in a few cells at the base of the vegetal pole by 18 hpf by WMISH
206 (Fig. S4B1, S4E1, and S1F). Of these three genes, *scl* was the first to show O-A NSM polarity
207 followed by *gatac* (Fig. S1B5, S1E5, and S1F5). Surprisingly, by 36 hpf *prox* did not exhibit spatial
208 distribution of transcripts that unambiguously indicated O-A polarity (Fig. S1E2-S1E5 and Fig.

209 S4E6), suggesting that either *prox* is a general mesodermal regulatory factor in *E. tribuloides* or it
210 is spatially restricted later in gastrular development.

211 These data on spatial dynamics of NSM regulatory factors suggest that there exist
212 numerous regulatory states in the anterior archenteron. To provide some clarity, double fluorescent
213 WMISH (dfWMISH) indicated this was indeed the case. Previous observations suggested that *E.*
214 *tribuloides* mesodermal domains broadly express *ets1/2* and *tbrain* (17), and dfWMISH confirmed
215 this result (Fig. S4IS4I). Within this broad *ets1/2-tbrain* domain, three regulatory states are
216 identified (Fig. S4G-S4I): (1) orally localized *ets1/2, tbrain* and *ese*; (2) aborally localized *ets1/2,*
217 *tbrain,* and *gcm*; and (3) an anteriorly localized micromere-descendant regulatory state at the tip of
218 the archenteron of *ets1/2, tbrain, ese* and *alx1.* The only similarity between NSM regulatory states
219 of *E. tribuloides* and that of euechinoids is *ese* is restricted to oral NSM and *gcm* to aboral NSM
220 (27). The NSM regulatory states described here make it clear that since the divergence of
221 cidaroids and euechinoids there have been numerous changes to spatial and temporal gene
222 expression during the early patterning of echinoid NSM cell types.

223 Perturbation of Nodal signaling suggests highly conserved 224 regulatory interactions in patterning echinoid O-A ectoderm and 225 mesoderm

226 Next we sought to experimentally perturb O-A specification in *E. tribuloides* to determine the
227 extent to which this developmental program is conserved in echinoids. In euechinoids, perturbation
228 of animal-vegetal (A-V) axis polarity by disruption of nuclearization of β-catenin indirectly disrupts
229 O-A axis specification (31, 33). One mechanism underlying the crosstalk of these two
230 deuterostome specification events was found to be restriction of *foxq2* to ANE, as its presence in
231 OE blocked *nodal* transcription (23). In *E. tribuloides,* disrupting nuclearization of β-catenin at the

232 vegetal pole by overexpressing dn-Cadherin RNA led to upregulation of *foxq2* and strong
233 downregulation of *nodal* and its euechinoid downstream components *bmp2/4, not,* and *tbx2/3* (Fig.
234 S5A). This result suggests that the molecular crosstalk between β-catenin/TCF, *foxq2* and *nodal*
235 are conserved in echinoids.

236 Next, we aimed to determine the spatiotemporal effects of perturbation of O-A specification
237 by culturing *E. tribuloides* embryos in the presence of SB43152, a small molecule antagonist of the
238 TGF-β (Nodal) receptor Alk4/5/7 (73). At four days post fertilization, these embryos exhibited
239 strong aboralization, archenterons that failed to make contact with OE, and supernumerary skeletal
240 elements (Fig. S5B). Quantitative PCR (qPCR) analysis at four different timepoints in *E. tribuloides*
241 development showed strong downregulation of OE regulatory factors *chordin, gsc, lefty, nodal* and
242 *not* (Fig. 2A). This result was confirmed spatially by WMISH for mRNA transcripts of *chordin, nodal*
243 and *not* (Fig. 2B and S5C). Another critical OE regulatory gene is the secreted TGF-β ligand
244 *bmp2/4.* This gene was clearly not affected to the same degree as the aforementioned cohort of
245 OE factors (Fig. 2A). This result is strikingly different from the strong downregulation of *bmp2/4*
246 observed in the euechinoid *P. lividus* when it was cultured in the presence of SB431542 or when
247 injected with Nodal morpholino (MASO) (38, 40), indicating that regulation of *bmp2/4* may be under
248 alternative control in *E. tribuloides*.

249 On the aboral side, a striking difference is the effect of SB431542 on *tbx2/3.* In euechinoids,
250 *tbx2/3* is downstream of *bmp2/4* ligand, which diffuses from OE to AE (58, 59, 74). Treatment of *P.*
251 *lividus* embryos with SB431542 inhibitor completely and specifically extinguishes *tbx2/3* in AE
252 while not interfering with its SM expression (40). In *E. tribuloides,* qPCR data suggest SB431542
253 inhibitor has no effect on *tbx2/3* regulation (Fig. 5C). However, WMISH of *tbx2/3* in the presence of
254 the inhibitor revealed its domain of expression had expanded into an equatorial ring (Fig. 2B and
255 S5C). Similarly, whereas in *E. tribuloides* qPCR data indicate strong downregulation of the AE

256 regulatory factor *irxa* (Fig. 5C), its domain of expression expanded into OE in *P. lividus* embryos
257 upon SB431542 treatment (40). These results suggest GRN architecture immediately downstream
258 of the initial *nodal* and *bmp2/4* circuitry has diverged in echinoids and further indicate that
259 regulatory interactions immediately upstream of *bmp2/4, irxa* and *tbx2/3* are regulated differently in
260 *E. tribuloides.*

261 Between the OE and AE is the pro-neural ciliary band that expresses *onecut.* In
262 euechinoids, perturbation of Nodal signaling results in an expansion of *onecut* throughout the
263 ectoderm, leading to the suggestion that the default fate of ectoderm is a pro-neural CB territory
264 (40). When this perturbation was carried out in *E. tribuloides,* a very different result was obtained in
265 which we see *onecut* restricted to a single equatorial band of 6-10 cell diameters (Fig. 2C). A
266 previous study showed that disruption of *E. tribuloides* endomesoderm formation by treatment with
267 zinc results in embryos exhibiting a ring of highly concentrated proneural synaptotagmin-B positive
268 cells at the equator of the embryo (75). Together, these observations indicate that, in the absence
269 of Nodal signaling, there are anteriorly positioned repressors in *E. tribuloides* restricting CB fate to
270 the equator of the embryo and that CB restriction from the ANE is functioning differently in
271 cidaroids and euechinoids.

272 Lastly, in euechinoids studied thus far, polarity in NSM (47) lineages is downstream of
273 Nodal signaling via the transcription factor Not (27, 71). In *E. tribuloides,* qPCR data did not
274 indicate consistent differences in mRNA abundance for NSM regulatory genes (Fig. 2A). However,
275 WMISH assays revealed that embryos treated with SB431542 failed to restrict *gcm* to the aboral
276 side (Fig. 2B and S5C). This observation is consistent with the euechinoid GRN linkage
277 immediately downstream of Nodal signaling via the transcription factor *not,* which represses aboral
278 NSM in the oral-facing region of the archenteron (27). Indeed, in *E. tribuloides, not* is seen in the
279 archenteron throughout gastrulation (Fig. 1J3-1J5). These observations are consistent with a

280 conserved role for Nodal signaling via *not* in establishing polarity in NSM cell types in the
281 archenteron of *E. tribuloides.*

282 Regulatory interactions establishing ciliary band are conserved in 283 echinoids

284 The spatial distributions of *gsc, onecut* and *irxa* are highly suggestive of a conserved
285 regulatory apparatus that spatially restricts CB to the boundary of OE and AE (Fig. 1 and Fig. S3).
286 Supporting this claim, microinjection of mutated or wild-type BACs encoding the *cis*-regulatory
287 region of *S. purpuratus onecut* and a GFP reporter were examined in *E. tribuloides*. In *S.*
288 *purpuratus, onecut* is restricted to the progenitor CB territory by *gsc* repression in OE and *irxa*
289 repression in AE (Fig. 3A). Recently, Barsi and Davidson (2016) experimentally validated four cis-
290 regulatory modules directing the activation of *onecut* by *soxb1* and repression of *onecut* by *gsc* in
291 OE and *irxa* in AE (Fig. 3B). Remarkably, these BACs faithfully recapitulated the regulatory activity
292 of these BACs in *E. tribuloides* (Fig. 3C-3H and Fig. S6). To test for this conservation, we assayed
293 a series of endogenous and site-directed mutagenesis *onecut* BACs from *S. purpuratus* by
294 microinjection (65). Remarkably, a BAC that has been shown to recapitulate the endogenous *S.*
295 *purpuratus onecut* expression pattern faithfully expressed reporter GFP in the CB of *E. tribuloides*
296 (Fig. 3H and S6A-S6B). Further, a BAC harboring mutated repressor sites for the oral repressor
297 *gsc* repeatedly exhibited ectopic expression in OE of *E. tribuloides* (Fig. 3E). When interpreted with
298 the spatial WMISH data of Figure 1, the early specification of CB regulatory factors suggests
299 divergence of initial activation of *onecut* and conserved GRN circuitry guiding the restriction of
300 *onecut* to CB territory by *irxa* and *gsc,* a striking example of a highly conserved developmental
301 program after 268 million years of evolution.

302 **Comparative analyses of temporal gene expression in echinoids**
303 **suggests ectodermal and mesodermal GRNs have diverged at**
304 **different rates**

305 The spatiotemporal data presented thus far are highly suggestive that O-A axis
306 specification, as well as gastrular CB formation, in *E. tribuloides* is consistent with similar
307 processes in euechinoids and that NSM specification has ostensibly diverged. Next we sought a
308 comparative gene expression approach to reveal the extent of divergence between echinoid
309 clades. We compared absolute mRNA transcript abundance of 18 regulatory genes in three
310 species and 55 *S. purpuratus* regulatory genes (76) in early euechinoid developmental GRNs for
311 14 early developmental timepoints in *E. tribuloides* (Table S5 and S6). We scaled timepoints from
312 *E. tribuloides* to the euechinoid *P. lividus* since both develop at a similar temperature and since
313 scaling of developmental stages between *P. lividus* and *S. purpuratus* had been previously
314 established (Table S5) (77). This allowed pairwise analyses of Spearmann's rank correlation
315 coefficients, ρ, between the three species were conducted (Table S6). Plotting relative mRNA
316 transcriptional dynamics for the three species were indicative of compelling correlation for
317 ectodermal regulatory factors and supported the notion of poor correlation for regulatory factors
318 driving mesoderm specification (Fig. 4 and S7). We next considered timecourse expression data of
319 55 orthologs of *E. tribuloides* and *S. purpuratus.* We binned the orthologs in ectoderm, endoderm
320 and mesoderm based on their spatial distributions in *S. purpuratus* and compared them against the
321 mean of all ρ values. Regulatory orthologs expressed in endoderm and ectoderm exhibited
322 significantly higher ρ relative to the mean of all ρ values, suggesting strong conservation of
323 transcriptional dynamics of these factors in echinoids (Fig. 5A). However, regulatory orthologs
324 expressed in mesodermal cell lineages did not depart significantly from the mean ρ, suggesting

325 transcriptional dynamics of mesodermal regulatory factors have changed markedly since the
326 cidaroid-euechinoid divergence (Fig. 5A and 5B). Furthermore, we conducted a comparative
327 clustering analysis to identify statistical differences in the timecourse data. By clustering *S.*
328 *purpuratus* regulatory orthologs into six distinct clusters and forcing assignment of each *E.*
329 *tribuloides* ortholog into all clusters, we acquired cluster membership scores and clustering
330 similarities for each ortholog (Table S7, S8, and S9). Considering *S. purpuratus* orthologs alone
331 revealed regulatory genes clustering together based on whether they are expressed maternal,
332 early or late in development (Fig. S8A). When *E. tribuloides* orthologs were forced into these *S.*
333 *purpuratus* clusters and the highest membership value for each ortholog was averaged with other
334 orthologs expressed in each germ layer, *E. tribuloides* orthologs expressed in ectodermal domains
335 exhibited higher cluster membership scores than orthologs expressed in mesodermal domains
336 (Fig. 5C, $p<0.05$, Mann-Whitney U Test). Additionally, ectodermal orthologs jumped less
337 frequently between clusters than mesodermal orthologs, suggesting timecourse data for
338 ectodermal genes were more similar than those mesodermal genes (Fig. 5D and S8C). These
339 analyses suggest that deployment of ectodermal regulatory genes is more similar between
340 euechinoids and cidaroids than deployment of mesodermal regulatory genes. Further,
341
342

343 Discussion

344 Extensive divergence of ectodermal and mesodermal regulatory 345 linkages has occurred in echinoid developmental GRNs

346 This study investigated embryonic pattern formation and regulatory interactions of the
347 euechinoid ectodermal and mesodermal GRNs in a distantly related cidaroid. By contrasting our

348 findings with regulatory diagram of the *S. purpuratus* developmental GRN, we are able to better
349 understand how the regulatory interactions patterning the early embryo have diverged since the
350 cidaroids and euechinoids last shared a common ancestor in the Paleozoic 268.8 mya (Fig. 6).
351 Numerous regulatory interactions were found to have diverged in these two clades, including (Fig
352 6A). Statistical analyses of comparative timecourse gene expression data revealed that gene
353 expression profiles of regulatory gene orthologs expressed in ectodermal cell lineages are more
354 similar to their euechinoid counterparts than those expressed in mesodermal cell lineages. This
355 result is consistent the with the broad differences observed in cidaroids regarding SM specification,
356 as well as that revealed here in NSM segregation and regulatory states. By contrasting these
357 observations with those in other echinoderms, we can begin to appreciate the degree to which
358 embryonic developmental GRNs are constrained or altered over vast evolutionary distances and
359 can reconstruct the ancestral regulatory states that must have existed in the embryos of
360 echinoderm ancestors (47). In the following we attempt to interpret the preceding results in an
361 evolutionary context within the echinoderm phylum.

362 Divergent regulatory interactions in the evolution of echinoid ectodermal and 363 mesodermal GRNs

364 Our analysis utilized the regulatory transactions of the well-known *S. purpuratus* GRN as a
365 basis for comparison between the cidaroid *E. tribuloides* and euechinoids (Fig. 6A). The
366 comparative approach combined with the well-documented fossil record of echinoids allowed us to
367 reveal a first approximation of the magnitude of change incurred by these GRNs since these two
368 clades last shared a common ancestor. Spatiotemporal expression patterns of ectodermal
369 regulatory genes in *E. tribuloides* and euechinoids strongly suggest that alteration to this circuitry is
370 nontrivial in early development relative to the circuitry directing development of mesodermal
371 lineages. However, while numerous regulatory transactions are conserved in the ectodermal GRN,

372 deployment and rewiring of circuitry during the evolution of euechinoid lineages that possess
373 direct-developing, non-feeding larvae has occurred frequently (52, 78-80). And as we have seen
374 from this study, our data indicate that the ectodermal GRN has undergone at least one significant
375 alteration since the cidaroid-euechinoid divergence, viz. the *bmp2/4, tbx2/3* and *irxa.* These
376 observations support the idea that the constraints on alteration of GRN circuitry are not sufficient to
377 maintain these linkages over vast evolutionary timescales. For instance, perturbation of Nodal
378 signaling revealed that, while initial specification events are highly similar, alterations likely have
379 occurred to the regulation of *bmp2/4* and *tbx2/3.* In *E. tribuloides tbx2/3* is expressed in AE and
380 aboral NSM by mid-gastrula. By late gastrula, it is expressed in the lateral clusters of skeletogenic
381 synthesis, at the tip of the gut, in the gut endoderm, and residually in the ectoderm. This unfolding
382 pattern of *tbx2/3* expression in *E. tribuloides* has essentially been compressed into the early stages
383 of euechinoid development (60). In euechinoids, perturbation of Nodal signaling with SB431542
384 extinguishes aboral ectodermal *tbx2/3* specifically in *P. lividus*, while not affecting its expression in
385 SM (40). In *E. tribuloides* we observed the expression domain of *tbx2/3* expand into OE upon
386 perturbation with this inhibitor (Fig. 2B and S5C). This observation combined with the result that
387 *bmp2/4* responds differently to Nodal perturbation suggests altered GRN circuitry downstream of
388 Nodal.

389 Evolution of ciliary band patterning mechanisms in echinoderms

390 Ciliary band formation and ANE patterning in *E. tribuloides* are evolutionarily interesting
391 given their position in the echinoderm phylogeny and given that cidaroids lack the pan-
392 deuterostome apical senory organ (12, 13, 81, 82). Previous studies indicated that ANE patterning
393 in *E. tribuloides* is more similar to outgroup echinoderms than it is in euechinoids; though
394 expression of CB and anterior regulatory factors, e.g. *onecut* and *nk2.1,* exhibited spatial
395 distributions similar to those seen in euechinoids (75). Here, we observed patterning and

396 regulation of CB that are consistent with the hypothesis that this process is conserved in echinoids
397 (Fig. 6B). Additionally, we observed the sequential spatial restriction of *foxq2* to ANE, a pan-
398 bilaterian observation driven by endomesodermal *wnt* factors (23, 83-86). These data suggest that
399 specification of the apical sensory organ in *E. tribuloides* is developmentally downstream of these
400 events and that the loss of this embryonic structure had little effect on conserved patterning of CB
401 and anterior localization of *foxq2*.
402

403 **Regulatory states and polarity of NSM in *E. tribuloides***

404 Examining mesodermal polarity in euechinoids and outgroup echinoderms aids in the
405 establishment of a timeline of GRN evolution. In euechinoid mesodermal NSM, *gcm* is directly
406 downstream of Notch signaling and later is restricted prior to gastrulation to aboral NSM by Not,
407 which is directly downstream of Nodal/SMAD signaling (37, 71, 87, 88). In cidaroids, early
408 expression of *gcm* is not dependent on Delta/Notch [Erkenbrack, Davidson and Peter, forthcoming]
409 and its mesodermal polarity is only apparent 4-6 hours after gastrulation has begun. Thus, if *gcm* is
410 near the top of the NSM GRN in cidaroids (16), as is the case in euechinoids (88), then this
411 pregastrular NSM polarization can be viewed as a euechinoid synapomorphy. This hypothesis is
412 supported by the observation that no significant polarity occurs in mesodermal specification of
413 asteroids and holothuroids (89). Here we showed that the polarization of *gcm* and *ese* also seems
414 to be a derived feature of echinoids and the mechanism of NSM segregation via Nodal/SMAD
415 signaling is likely conserved (Fig. 6C). Two observations make *gcm* polarization via the
416 transcription factor *not* (27) likely to exist in *E. tribuloides*: (1) *not* expression is observed in the oral
417 side of the archenteron by early gastrula stage when *gcm* is spatially restricted (Fig. 1J4 and 1L3)
418 and (2) aboral localization of *gcm* does not obtain when O-A axis patterning, and thereby *not*
419 expression, is perturbed (Fig. 2B and S5C). Together these observations suggest a conserved role

420 for OE regulatory factors in patterning the NSM of echinoids and that, in the lineage leading to
421 modern euechinoids, deployment of GRN circuitry polarizing NSM underwent a heterochronic shift
422 in the lineage leading to euechinoids.

423 The data presented on O-A polarity in the NSM of *E. tribuloides* suggest that multiple
424 regulatory domains unfold at and around the tip of the archenteron as gastrulation proceeds. This
425 is also the case in euechinoids (90). However, this study determined that *ese* operates in the oral
426 NSM exclusive of *gcm* in the aboral NSM. While the regulatory states in *E. tribuloides* NSM need
427 further refinement by two-color WMISH, for our purposes the overt disorder in its formation relative
428 to the overt order of *S. purpuratus* NSM makes two salient points. First, early pregastrular or early
429 gastrular polarity of NSM regulatory states represents an echinoid novelty, as no evidence for early
430 mesodermal polarity exists in outgroup echinoderms (89, 91). Second, if we take *E. tribuloides* as
431 a proxy to the ancestral state for this character/regulatory state, then it is clear that the O-A polarity
432 observed in the euechinoid NSM was shifted to occur prior to gastrulation in the lineage leading to
433 modern euechinoids. On the other hand, an alternative evolutionary scenario is that NSM polarity
434 manifested in these two modern echinoids is the result of two independent evolutionary trajectories
435 with heterochronic and spatial differences, but both meeting a similar end in the diversification of
436 NSM cell types in early development. That at least two O-A regulatory states are common to these
437 embryos and that *gcm* is downstream of Nodal and much later is downstream of Notch signaling
438 provide support for the first scenario. Further investigation into the developmental timing and
439 regulatory states of NSM segregation in *E. tribuloides* and other cidaroids is required to parse out
440 the most likely evolutionary scenario of NSM evolution in echinoids.

441

442 Evolution of global embryonic domains in early development of 443 echinoids

444 Previous analyses of embryonic regulatory states in *E. tribuloides* surveyed SM regulatory
445 factors (17, 47) and anterior neural ectoderm specification (75). Additionally, two previous studies
446 investigated SM and early endomesodermal micromere regulatory factors in the Pacific-dwelling
447 cidaroid *Prionocidaris baculosa* (16, 92). Integrating these data into this study affords an analysis
448 of global embryonic regulatory states and GRN linkages over 268.8 mya of evolution in indirect-
449 developing sea urchins. From these studies, numerous alterations to deployment and GRN
450 circuitry at all levels of GRN topology can be enumerated. Here, we enumerate 19 changes in
451 spatiotemporal deployment or regulation of ectodermal and mesodermal embryonic regulatory
452 factors since the cidaroid-euechinoid divergence (Table S1). Prominent among alterations of
453 regulatory interactions are those that have occurred in establishing polarity in mesodermal
454 embryonic domains. Endodermal and ectodermal specification and regulatory states also have
455 undergone significant change, but to a lesser degree. One hypothesis that can accommodate
456 these observations is that endodermal and ectodermal developmental programs may be more
457 recalcitrant to change than mesodermal programs due to their more ancient evolutionary origin (5),
458 suggesting that accretion of process over evolutionary time is a mechanism of constraint in
459 developmental programs (5). Indeed, in euechinoids there have been additional layers of GRN
460 topology accrued in mesodermal specification, e.g. the *pmar1-hesc* double-negative gate novelty
461 (16, 17, 22), delta-dependent NSM specification (17, 34), etc., which cidaroids do not exhibit, and
462 which may explain the observation that little to no appreciable change has been observed in the
463 mesodermal developmental programs of *L. variegatus, P. lividus* and *S. purpuratus,*
464 representatives of modern euechinoid lineages that diverged approximately 90 mya.

465 Since the divergence of cidaroids and euechinoids, numerous alterations to developmental
466 GRNs have accrued in these lineages. This study revealed that changes to mesodermal GRN
467 architecture have occurred more frequently than alterations to ectoderm GRN architecture. These

468 results support the notion that GRN architecture evolves at different rates (93) and provide an in
469 principle explanation for the rapid evolution observed in both cidaroid and euechinoid sea urchin
470 lineages that have independently evolved direct-developing larval forms (53). It remains to be
471 determined by future research efforts whether the shared regulatory states between cidaroids and
472 euechinoids elucidated here are the product of conserved stretches of genomic DNA hardwired in
473 the *cis*-regulatory regions of the orthologous regulatory genes or whether they are the result of
474 diverged *cis*-regulatory modules producing similar developmental outcomes.

475 Materials and Methods

476 Animal and embryo culture, cloning, acquisition of spatial and temporal gene expression data and
477 microinjection perturbation data were as previously described (17, 47). Dosage of small molecule
478 inhibitors DAPT and SB431542 were determined by dilution series. Concentrations for DAPT and
479 SB431542 were 12 μM and 15 μM respectively. Additional details for previously described
480 methods, statistical analyses and all other experimental manipulations can be found in SI Materials
481 and Methods.

482 Acknowledgments

483 We appreciatively acknowledge numerous colleagues for discussing various aspects of this work
484 with us over the long course of its maturation: Dr. Julius C. Barsi kindly provided his knowledge
485 and the *Sp onecut* engineered BACs; Jennifer Wellman, M.S., for her insight on statistical
486 analyses; Stefan Materna provided raw data for *S. purpuratus* mRNA transcript abundance and
487 reviewed early versions of the manuscript; Matthias Futschik provided mfuzz analysis advice; Drs.
488 Oliver Griffith, David McClay, Tom Stewart and Jeffrey R. Thompson provided critical commentary
489 on figures and the manuscript. The commentary of two anonymous reviewers greatly improved
490 data analysis and the manuscript. This work was developed and written in the laboratory of
491 Professor Günter P. Wagner; his patience and support are fondly appreciated. This work was
492 funded by National Science Foundation CREATIV grant #1240626.
493

494 References

1. Davidson EH (1986) *Gene activity in early development* (Academic Press, New York) 3rd Ed.
2. Wikramanayake AH*, et al.* (2003) An ancient role for nuclear beta-catenin in the evolution of axial polarity and germ layer segregation. *Nature* 426(6965):446-450.
3. Davidson EH (2006) *The regulatory genome: gene regulatory networks in development and evolution* (Academic, Oxford).
4. Peter IS & Davidson EH (2015) *Genomic Control Process, Development and Evolution* (Academic Press, Oxford).
5. Hashimshony T, Feder M, Levin M, Hall BK, & Yanai I (2015) Spatiotemporal transcriptomics reveals the evolutionary history of the endoderm germ layer. *Nature* 519(7542):219-222.
6. Davidson EH (1991) Spatial mechanisms of gene regulation in metazoan embryos. *Development* 113(1):1-26.
7. Davidson EH, Cameron RA, & Ransick A (1998) Specification of cell fate in the sea urchin embryo: summary and some proposed mechanisms. *Development* 125(17):3269-3290.
8. Wray GA & Bely AE (1994) The evolution of echinoderm development is driven by several distinct factors. *Development* 1994(Supplement):97-106.
9. Kroh A & Smith AB (2010) The phylogeny and classification of post-Palaeozoic echinoids. *J Syst Palaeontol* 8(2):147-212.
10. Thompson JR*, et al.* (2015) Reorganization of sea urchin gene regulatory networks at least 268 million years ago as revealed by oldest fossil cidaroid echinoid. *Sci Rep-Uk* 5.
11. Tennent D (1914) The early influence of the spermatazoan upon the characters of echinoid larvae. *Carn. Inst. Wash. Publ.* 182:129-138.
12. Mortensen T (1938) Contributions to the study of the development and larval forms of echinoderms. IV. *Danske Vid. Selsk. Ser.* 9(7(3)):1-59.
13. Schroeder TE (1981) Development of a 'primitive' sea urchin (Eucidaris tribuloides): irregularities in the hyaline layer, micromeres, and primary mesenchyme. *Biological Bulletin* 161(1):141-151.
14. Wray GA & McClay DR (1988) The origin of spicule-forming cells in a 'primitive' sea urchin (Eucidaris tribuloides) which appears to lack primary mesenchyme cells. *Development* 103(2):305-315.
15. Wray GA & McClay DR (1989) Molecular heterochronies and heterotopies in early echinoid development. *Evolution*:803-813.
16. Yamazaki A, Kidachi Y, Yamaguchi M, & Minokawa T (2014) Larval mesenchyme cell specification in the primitive echinoid occurs independently of the double-negative gate. *Development* 141(13):2669-2679.
17. Erkenbrack EM & Davidson EH (2015) Evolutionary Rewiring of Gene Regulatory Network Linkages at Divergence of the Echinoid Subclasses. *PNAS*.
18. Gao F*, et al.* (2015) Juvenile skeletogenesis in anciently diverged sea urchin clades. *Dev Biol* 400(1):148-158.
19. Angerer LM*, et al.* (2000) A BMP pathway regulates cell fate allocation along the sea urchin animal-vegetal embryonic axis. *Development* 127(5):1105-1114.
20. Davidson EH*, et al.* (2002) A genomic regulatory network for development. *Science* 295(5560):1669-1678.
21. Revilla-i-Domingo R, Oliveri P, & Davidson EH (2007) A missing link in the sea urchin embryo gene regulatory network: hesC and the double-negative specification of micromeres. *Proc Natl Acad Sci U S A* 104(30):12383-12388.

542 22. Oliveri P, Tu Q, & Davidson EH (2008) Global regulatory logic for specification of an
543 embryonic cell lineage. *Proc Natl Acad Sci U S A* 105(16):5955-5962.
544 23. Yaguchi S, Yaguchi J, Angerer RC, & Angerer LM (2008) A Wnt-FoxQ2-nodal pathway links
545 primary and secondary axis specification in sea urchin embryos. *Developmental cell*
546 14(1):97-107.
547 24. Su Y-H*, et al.* (2009) A perturbation model of the gene regulatory network for oral and
548 aboral ectoderm specification in the sea urchin embryo. *Developmental biology* 329(2):410-
549 421.
550 25. Peter IS & Davidson EH (2010) The endoderm gene regulatory network in sea urchin
551 embryos up to mid-blastula stage. *Dev Biol* 340(2):188-199.
552 26. Peter IS & Davidson EH (2011) A gene regulatory network controlling the embryonic
553 specification of endoderm. *Nature* 474(7353):635-639.
554 27. Materna SC, Ransick A, Li E, & Davidson EH (2013) Diversification of oral and aboral
555 mesodermal regulatory states in pregastrular sea urchin embryos. *Dev Biol* 375(1):92-104.
556 28. Barsi JC, Li EH, & Davidson EH (2015) Geometric control of ciliated band regulatory states
557 in the sea urchin embryo. *Development* 142(5):953-961.
558 29. Nam JM*, et al.* (2008) Cis-regulatory control of the nodal gene, initiator of the sea urchin oral
559 ectoderm gene network. *Faseb J* 22.
560 30. Cui M, Siriwon N, Li E, Davidson EH, & Peter IS (2014) Specific functions of the Wnt
561 signaling system in gene regulatory networks throughout the early sea urchin embryo.
562 *Proceedings of the National Academy of Sciences* 111(47):E5029-E5038.
563 31. Wikramanayake AH, Huang L, & Klein WH (1998) beta-Catenin is essential for patterning
564 the maternally specified animal-vegetal axis in the sea urchin embryo. *P Natl Acad Sci USA*
565 95(16):9343-9348.
566 32. Sherwood DR & McClay DR (1999) LvNotch signaling mediates secondary mesenchyme
567 specification in the sea urchin embryo. *Development* 126(8):1703-1713.
568 33. Logan CY, Miller JR, Ferkowicz MJ, & McClay DR (1999) Nuclear beta-catenin is required
569 to specify vegetal cell fates in the sea urchin embryo. *Development* 126(2):345-357.
570 34. Sweet HC, Gehring M, & Ettensohn CA (2002) LvDelta is a mesoderm-inducing signal in the
571 sea urchin embryo and can endow blastomeres with organizer-like properties. *Development*
572 129(8):1945-1955.
573 35. Flowers VL, Courteau GR, Poustka AJ, Weng W, & Venuti JM (2004) Nodal/activin signaling
574 establishes oral–aboral polarity in the early sea urchin embryo. *Developmental dynamics*
575 231(4):727-740.
576 36. Ettensohn CA, Kitazawa C, Cheers MS, Leonard JD, & Sharma T (2007) Gene regulatory
577 networks and developmental plasticity in the early sea urchin embryo: alternative
578 deployment of the skeletogenic gene regulatory network. *Development* 134(17):3077-3087.
579 37. Croce JC & McClay DR (2010) Dynamics of Delta/Notch signaling on endomesoderm
580 segregation in the sea urchin embryo. *Development* 137(1):83-91.
581 38. Duboc V, Rottinger E, Besnardeau L, & Lepage T (2004) Nodal and BMP2/4 signaling
582 organizes the oral-aboral axis of the sea urchin embryo. *Developmental Cell* 6(3):397-410.
583 39. Duboc V, Lapraz F, Besnardeau L, & Lepage T (2008) Lefty acts as an essential modulator
584 of Nodal activity during sea urchin oral-aboral axis formation. *Developmental Biology*
585 320(1):49-59.
586 40. Saudemont A*, et al.* (2010) Ancestral Regulatory Circuits Governing Ectoderm Patterning
587 Downstream of Nodal and BMP2/4 Revealed by Gene Regulatory Network Analysis in an
588 Echinoderm. *Plos Genet* 6(12).

589 41. Lhomond G, McClay DR, Gache C, & Croce JC (2012) Frizzled1/2/7 signaling directs beta-
590 catenin nuclearisation and initiates endoderm specification in macromeres during sea urchin
591 embryogenesis. *Development* 139(4):816-825.
592 42. Cavalieri V & Spinelli G (2014) Early asymmetric cues triggering the dorsal/ventral gene
593 regulatory network of the sea urchin embryo. *Elife* 3:e04664.
594 43. Smith AB*, et al.* (2006) Testing the molecular clock: molecular and paleontological estimates
595 of divergence times in the Echinoidea (Echinodermata). *Mol Biol Evol* 23(10):1832-1851.
596 44. Croce J*, et al.* (2011) Wnt6 activates endoderm in the sea urchin gene regulatory network.
597 *Development* 138(15):3297-3306.
598 45. Ettensohn CA (2009) Lessons from a gene regulatory network: echinoderm skeletogenesis
599 provides insights into evolution, plasticity and morphogenesis. *Development* 136(1):11-21.
600 46. Molina MD, de Croze N, Haillot E, & Lepage T (2013) Nodal: master and commander of the
601 dorsal-ventral and left-right axes in the sea urchin embryo. *Current Opinion in Genetics &*
602 *Development* 23(4):445-453.
603 47. Erkenbrack EM*, et al.* (2016) Ancestral state reconstruction by comparative analysis of a
604 GRN kernel operating in echinoderms. *Dev Genes Evol* 226(1):37-45.
605 48. Lapraz F, Haillot E, & Lepage T (2015) A deuterostome origin of the Spemann organiser
606 suggested by Nodal and ADMPs functions in Echinoderms. *Nat Commun* 6:8927.
607 49. Duboc V & Lepage T (2008) A conserved role for the nodal signaling pathway in the
608 establishment of dorso-ventral and left-right axes in deuterostomes. *J Exp Zool Part B*
609 310b(1):41-53.
610 50. Wray GA & Raff RA (1991) The evolution of developmental strategy in marine invertebrates.
611 *Trends Ecol Evol* 6(2):45-50.
612 51. Smith MS, Collins S, & Raff RA (2009) Morphogenetic mechanisms of coelom formation in
613 the direct-developing sea urchin Heliocidaris erythrogramma. *Dev Genes Evol* 219(1):21-29.
614 52. Smith MS, Turner FR, & Raff RA (2008) Nodal Expression and Heterochrony in the
615 Evolution of Dorsal-Ventral and Left-Right Axes Formation in the Direct-Developing Sea
616 Urchin Heliocidaris erythrogramma. *J Exp Zool Part B* 310b(8):609-622.
617 53. Raff RA (2008) Origins of the other metazoan body plans: the evolution of larval forms.
618 *Philos T R Soc B* 363(1496):1473-1479.
619 54. Su Y-H (2009) Gene regulatory networks for ectoderm specification in sea urchin embryos.
620 *Biochimica et Biophysica Acta (BBA)-Gene Regulatory Mechanisms* 1789(4):261-267.
621 55. Li E, Cui M, Peter IS, & Davidson EH (2014) Encoding regulatory state boundaries in the
622 pregastrular oral ectoderm of the sea urchin embryo. *Proceedings of the National Academy*
623 *of Sciences* 111(10):E906-E913.
624 56. Li E, Materna SC, & Davidson EH (2012) Direct and indirect control of oral ectoderm
625 regulatory gene expression by Nodal signaling in the sea urchin embryo. *Dev Biol*
626 369(2):377-385.
627 57. Li E, Materna SC, & Davidson EH (2013) New regulatory circuit controlling spatial and
628 temporal gene expression in the sea urchin embryo oral ectoderm GRN. *Dev Biol*
629 382(1):268-279.
630 58. Lapraz F, Besnardeau L, & Lepage T (2009) Patterning of the Dorsal-Ventral Axis in
631 Echinoderms: Insights into the Evolution of the BMP-Chordin Signaling Network. *Plos*
632 *Biology* 7(11).
633 59. de-Leon SB-T, Su Y-H, Lin K-T, Li E, & Davidson EH (2013) Gene regulatory control in the
634 sea urchin aboral ectoderm: spatial initiation, signaling inputs, and cell fate lockdown.
635 *Developmental biology* 374(1):245-254.

636 60. Croce J, Lhomond G, & Gache C (2003) Coquillette, a sea urchin T-box gene of the Tbx2
637 subfamily, is expressed asymmetrically along the oral-aboral axis of the embryo and is
638 involved in skeletogenesis. *Mech Dev* 120(5):561-572.
639 61. Gross JM, Peterson RE, Wu SY, & McClay DR (2003) LvTbx2/3: a T-box family
640 transcription factor involved in formation of the oral/aboral axis of the sea urchin embryo.
641 *Development* 130(9):1989-1999.
642 62. Range R (2014) Specification and positioning of the anterior neuroectoderm in
643 deuterostome embryos. *genesis* 52(3):222-234.
644 63. Strathmann RR (1971) The feeding behavior of planktotrophic echinoderm larvae:
645 mechanisms, regulation, and rates of suspensionfeeding. *Journal of Experimental Marine*
646 *Biology and Ecology* 6(2):109-160.
647 64. Wray GA (1992) The Evolution of Larval Morphology during the Postpaleozoic Radiation of
648 Echinoids. *Paleobiology* 18(3):258-287.
649 65. Barsi JC & Davidson EH (2016) cis-Regulatory control of the initial neurogenic pattern of
650 onecut gene expression in the sea urchin embryo. *Developmental Biology* 409(1):310-318.
651 66. Poustka AJ*, et al.* (2007) A global view of gene expression in lithium and zinc treated sea
652 urchin embryos: new components of gene regulatory networks. *Genome Biol* 8(5):R85.
653 67. Otim O, Amore G, Minokawa T, McClay DR, & Davidson EH (2004) SpHnf6, a transcription
654 factor that executes multiple functions in sea urchin embryogenesis. *Dev Biol* 273(2):226-
655 243.
656 68. Cameron RA & Davidson EH (1991) Cell type specification during sea urchin development.
657 *Trends Genet* 7(7):212-218.
658 69. Sweet HC, Hodor PG, & Ettensohn CA (1999) The role of micromere signaling in Notch
659 activation and mesoderm specification during sea urchin embryogenesis. *Development*
660 126(23):5255-5265.
661 70. Materna SC & Davidson EH (2012) A comprehensive analysis of Delta signaling in pre-
662 gastrular sea urchin embryos. *Dev Biol* 364(1):77-87.
663 71. Duboc V*, et al.* (2010) Nodal and BMP2/4 pattern the mesoderm and endoderm during
664 development of the sea urchin embryo. *Development* 137(2):223-235.
665 72. Lee PY & Davidson EH (2004) Expression of Spgatae, the Strongylocentrotus purpuratus
666 ortholog of vertebrate GATA4/5/6 factors. *Gene Expression Patterns* 5(2):161-165.
667 73. Duboc V, Rottinger E, Lapraz F, Besnardeau L, & Lepage T (2005) Left-right asymmetry in
668 the sea urchin embryo is regulated by nodal signaling on the right side. *Developmental Cell*
669 9(1):147-158.
670 74. Bradham CA*, et al.* (2009) Chordin is required for neural but not axial development in sea
671 urchin embryos. *Dev Biol* 328(2):221-233.
672 75. Bishop CD, MacNeil KE, Patel D, Taylor VJ, & Burke RD (2013) Neural development in
673 Eucidaris tribuloides and the evolutionary history of the echinoid larval nervous system. *Dev*
674 *Biol* 377(1):236-244.
675 76. Materna SC, Nam J, & Davidson EH (2010) High accuracy, high-resolution prevalence
676 measurement for the majority of locally expressed regulatory genes in early sea urchin
677 development. *Gene Expr Patterns* 10(4-5):177-184.
678 77. Gildor T & de-Leon SB-T (2015) Comparative Study of Regulatory Circuits in Two Sea
679 Urchin Species Reveals Tight Control of Timing and High Conservation of Expression
680 Dynamics. *Plos Genet* 11(7):e1005435.
681 78. Wilson KA, Andrews ME, Turner FR, & Raff RA (2005) Major regulatory factors in the
682 evolution of development: the roles of goosecoid and Msx in the evolution of the direct-
683 developing sea urchin Heliocidaris erythrogramma. *Evolution & Development* 7(5):416-428.

79. Wilson KA, Andrews ME, & Raff RA (2005) Dissociation of expression patterns of homeodomain transcription factors in the evolution of developmental mode in the sea urchins Heliocidaris tuberculata and H-erythrogramma. *Evolution & Development* 7(5):401-415.
80. Raff RA & Smith MS (2009) Axis Formation and the Rapid Evolutionary Transformation of Larval Form. *Current Topics in Developmental Biology, Vol 86* 86:163-190.
81. Emlet RB (1988) Larval Form and Metamorphosis of a Primitive Sea-Urchin, Eucidaris-Thouarsi (Echinodermata, Echinoidea, Cidaroida), with Implications for Developmental and Phylogenetic Studies. *Biological Bulletin* 174(1):4-19.
82. Bennett KC, Young CM, & Emlet RB (2012) Larval Development and Metamorphosis of the Deep-Sea Cidaroid Urchin Cidaris blakei. *Biological Bulletin* 222(2):105-117.
83. Tu Q, Brown CT, Davidson EH, & Oliveri P (2006) Sea urchin Forkhead gene family: phylogeny and embryonic expression. *Dev Biol* 300(1):49-62.
84. Santagata S, Resh C, Hejnol A, Martindale MQ, & Passamaneck YJ (2012) Development of the larval anterior neurogenic domains of Terebratalia transversa (Brachiopoda) provides insights into the diversification of larval apical organs and the spiralian nervous system. *EvoDevo* 3(1):1.
85. Yu JK*, et al.* (2008) The Fox genes of Branchiostoma floridae. *Dev Genes Evol* 218(11-12):629-638.
86. Fritzenwanker JH, Gerhart J, Freeman RM, & Lowe CJ (2014) The Fox/Forkhead transcription factor family of the hemichordate Saccoglossus kowalevskii. *Evodevo* 5.
87. Ransick A, Rast JP, Minokawa T, Calestani C, & Davidson EH (2002) New early zygotic regulators expressed in endomesoderm of sea urchin embryos discovered by differential array hybridization. *Dev Biol* 246(1):132-147.
88. Ransick A & Davidson EH (2006) cis-regulatory processing of Notch signaling input to the sea urchin glial cells missing gene during mesoderm specification. *Dev Biol* 297(2):587-602.
89. McCauley BS, Wright EP, Exner C, Kitazawa C, & Hinman VF (2012) Development of an embryonic skeletogenic mesenchyme lineage in a sea cucumber reveals the trajectory of change for the evolution of novel structures in echinoderms. *Evodevo* 3(1):17.
90. Andrikou C, Pai CY, Su YH, & Arnone MI (2015) Logics and properties of a genetic regulatory program that drives embryonic muscle development in an echinoderm. *Elife* 4.
91. Dylus DV*, et al.* (2016) Large-scale gene expression study in the ophiuroid Amphiura filiformis provides insights into evolution of gene regulatory networks. *Evodevo* 7.
92. Yamazaki A, Kidachi Y, & Minokawa T (2012) "Micromere" formation and expression of endomesoderm regulatory genes during embryogenesis of the primitive echinoid Prionocidaris baculosa. *Dev Growth Differ* 54(5):566-578.
93. Davidson EH & Erwin DH (2006) Gene regulatory networks and the evolution of animal body plans. *Science* 311(5762):796-800.

Figure Legends

Fig 1. Spatiotemporal dynamics of eleven euechinoid ectodermal and mesodermal regulatory genes in the cidaroid *E. tribuloides*. Visualization of mRNA transcripts revealed by whole mount in situ hybridization, and estimates of absolute mRNA transcript abundance

727 determined by qPCR during first 35 hours post fertilization (hpf). Individual data points are light
728 grey. Blue data points represent the mean at that particular timepoint. Red dashed lines indicate
729 the onset of zygotic transcription. Orange asterisks denote position of archenteron. (A1) Key to
730 embryonic domains of expression and orientation of embryo micrographs. The embryonic domain
731 of expression of each gene is indicated by colored boxes: ANE (anterior neural ectoderm), pink;
732 oral ectoderm (OE), yellow; ciliary band (CB), blue; aboral ectoderm (AE), green; NSM (non-
733 skeletogenic mesoderm), brown. (B1-B5) Spatiotemporal expression of *foxq2. Foxq2* spatial
734 distribution is detected prior to hatching and is spatially restricted to ANE by 17 hpf. (C1-C5)
735 Spatiotemporal expression of *irxa.* At 28 hpf, *irxa* is detected in AE and extends from the vegetal
736 endodermal domains to ANE. By 40 hpf *irxa* is seen extending anteriorly at the boundary of AE
737 and OE. (D1-D5) Spatiotemporal expression of *nodal*. *Nodal* spatial distribution is restricted to a
738 few cells in OE up to early-mid gastrula stage. (E1-E5) Spatiotemporal expression of *chordin.* First
739 observed in a few cells in OE at 17 hpf, *chordin* subsequently expands to extend from the perianal
740 ectoderm to ANE. (F1-F5) Spatiotemporal dynamics of *msx.* Detected exclusively in AE, *msx*
741 extends from the blastopore to ANE. (G1-G5) Spatiotemporal expression of *gsc.* By 22 hpf, *gsc* is
742 detected in a broad region surrounding OE and later is observed around the stomodeum. (H1-H5)
743 Spatiotemporal dynamics of *onecut.* By 40 hpf *onecut* is detected in the future post oral ciliary
744 band and is initiated in a band moving from the posterior to the anterior. (I1-I5) Spatiotemporal
745 expression of *tbx2/3.* Spatial distribution of *tbx2/3* at 17 hpf is detected broadly in aboral ectoderm
746 (AE) and later extends from the perianal ectoderm to lateral AE, but not past the embryonic
747 equator. (J1-J5) Spatiotemporal expression of *not. Not* spatial distribution is first detected in a
748 similar field of cells as *nodal* and *lefty;* however, the domain of *not* subsequently expands by 28 hpf
749 where it is seen in the oral side of the archenteron, where non-skeletogenic mesoderm (NSM) and
750 endoderm are being segregated. By 40 hpf, the spatial domain of *not* extends from anterior neural

751 ectoderm to the perianal ectoderm, is clearly seen in NSM, and was not detected in endodermal
752 lineages. (K1-K5) Spatiotemporal expression of *ese. Ese* is detected primarily in non-skeletogenic
753 mesoderm (NSM) but also in anterior neural ectoderm. By 28 hpf, *ese* is observed at the tip of the
754 archenteron and is asymmetrically polarized in NSM. (L1-L5) Spatiotemporal expression of *gcm.*
755 As gastrulation begins *gcm* is expressed broadly in NSM; however by 28 hpf it exhibits stark
756 polarity in a field of cells that resides basal to the tip of the archenteron. *Gcm* is also observed in a
757 few ectodermal cells at the time of primary mesenchymal ingression.

758 **Fig 2. Perturbation of oral-aboral axis formation in *E. tribuloides* reveals alterations to**
759 **regulatory factor deployment in echinoids.** (A1) Quantitative effect of SB431542 on expression
760 of 30 *E. tribuloides* regulatory genes as revealed by qPCR. Fold change in mRNA transcripts
761 (ddCt) is shown on the y-axis. Two timepoints from two independent replicates are shown.
762 Regulatory factors are listed on the x-axis and font color designates their embryonic domain: pink,
763 anterior neural ectoderm; green, aboral ectoderm; yellow, oral ectoderm; black, endoderm; brown,
764 mesoderm. (B) WMISH of select ectodermal and mesodermal regulatory genes in embryos
765 cultured in the presence of SB431542. At 28 hpf expression of *chordin, nodal* and *not* are
766 completely extinguished. Whereas *gcm* is regularly restricted to one side of the archenteron, in the
767 presence of SB431542 it exhibits expression throughout the archenteron. In the ectoderm,
768 expression *tbx2/3* expands from aboral ectoderm (AE) into oral ectoderm in the presence of the
769 inhibitor. (C) The ciliary band marker *onecut* is normally observed in a band of cells between the
770 boundaries of OE and AE. However, in the presence of SB431542, *onecut* is expressed in an
771 equatorial band that is 6-10 cell diameters across.

772 **Fig 3. Expression dynamics in *E. tribuloides* of engineered reporter BACs harboring the**
773 **regulatory locus of *S. purpuratus onecut* suggest conservation of GRN circuitry positioning**
774 **ciliary band in echinoids** . (A) Schematic of ciliary band (CB) restriction in the *S. purpuratus*

775 embryo. Red bars indicate repressor genes restrict CB genes from expression in those domains.
776 (B) Schematic showing the *S. purpuratus onecut* locus and the *cis*-regulatory modules (CRMs)
777 responsible for the geometric positioning of *onecut.* (C) Table showing reporter analysis of spatial
778 expression of five engineered *S. purpuratus onecut* BACs in *E. tribuloides.* The BACs were
779 previously utilized to analyze the *cis*-regulatory dynamics of *onecut* spatial restriction in *S.*
780 *purpuratus* (Barsi and Davidson, 2016). (D) BAC reporter 1, which harbors mutations to all known
781 *cis*-regulatory modules (CRMs), showed a marked reduction of all reporter expression. (E) BAC
782 reporter 2 harbors mutations to a CRM driving zygotic activation. (F) BAC Reporter 4, which
783 harbors mutations to the aboral and oral ectodermal repression CRMs, increases the percent of
784 embryos that show reporter expression in the oral ectoderm, as well as normal reporter expression
785 in the ciliary band. (G) BAC reporter 3, which harbor mutated post-activation enhancer CRMs,
786 showed reduced reporter expression both in terms of percent embryos exhibiting reporter activity
787 and in the number of cells with reporter. (H) BAC Reporter 5, which harbors the unperturbed, wild-
788 type locus of *S. purpuratus onecut,* faithfully exhibits reporter GFP in the ciliary band domain of *E.*
789 *tribuloides.*

790 **Fig 4. Comparative gene expression analysis of echinoid regulatory orthologs.**
791 *Strongylocentrotus purpuratus,* purple line*; Paracentrotus lividus,* green dashed line; *Eucidaris*
792 *tribuloides,* black dashed line. Region of expression is indicated by a colored box. Transcripts per
793 embryo for each gene were normalized to their maximal expression over the first 30 hours of
794 development and are plotted against *E. tribuloides* development on the x-ordinate. Comparative
795 developmental staging for each species is listed in Table S5. Each analysis is accompanied by a
796 matrix of Spearman correlation coefficients (indicated as ρ).

797 **Fig 5. Statistical analyses of comparative timecourse data in the euechinoid *S. purpuratus***
798 **and the cidaroid *E. tribuloides.*** (A-B) Distribution plots of Spearman's rank correlation

799 coefficients (ρ) for temporal dynamics in *E. tribuloides* and *S. purpuratus*. Genes were binned by
800 embryonic domain of *S. purpuratus* spatial expression. Boxplot boundaries show interquartile
801 range, means and standard deviation. Asterisks mark statistical significance as determined by a
802 two-tailed t-test. (A) Boxplots for statistical distribution of endodermal, ectodermal and mesodermal
803 regulatory factors in *E. tribuloides* and *S. purpuratus.* Mean ρ for endodermal and ectodermal
804 regulatory factors were significantly higher than the mean ρ, marked as a red dashed line.
805 Mesodermal regulatory factors did not significantly vary from the mean. (B) Boxplots for statistical
806 distribution of subdomains of ectodermal and mesodermal regulatory factors in *E. tribuloides* and
807 *S. purpuratus.* (C) Mean mfuzz membership scores derived from cluster analysis of regulatory
808 orthologs. Genes were binned by their *S. purpuratus* embryonic domain of expression.
809 Membership scores for *E. tribuloides* orthologs were binned based on their spatial distribution and
810 compiled for statistical analysis. *E. tribuloides* ectodermal orthologs exhibited higher membership
811 scores than mesodermal orthologs (Mann Whitney U Test, $p<0.05$). (D) Histogram showing both
812 the distribution of tissue-specific orthologs examined in this study and the percent of *S. purpuratus*
813 and *E. tribuloides* orthologs clustering together. Ectodermal and endodermal orthologs clustered
814 together more often than mesodermal orthologs
815 **Fig 6. Modeling divergent and conserved regulatory transactions since the divergence of**
816 **cidaroids and euechinoids.** (A) A truncated *S. purpuratus* GRN showing ectodermal and
817 mesodermal regulatory interactions investigated in this study. Solid black lines indicated conserved
818 interactions; dashed black lines indicate interactions that are likely conserved; solid red lines
819 indicate divergent regulatory interactions. Genes and their *cis*-regulatory regions are represented
820 as flat lines with arrows. Embryonic domains of the echinoid embryo are represented by large
821 boxes: pink, anterior neural ectoderm (ANE); yellow, oral ectoderm (OE); blue, ciliary band (CB);
822 green, aboral ectoderm (AE); brown, oral non-skeletogenic mesoderm (NSM); light brown, aboral

823 non-skeletogenic mesoderm (NSM); white, skeletogenic mesoderm (SM). (B) Regulatory states
824 and restriction of ectodermal CB in asteroids, cidaroids and euechinoids. Red bars indicate
825 repressor genes restrict CB in a particular embryonic domain. Color scheme is the same as in (A).
826 The top row of schematics represents the wild-type state in three echinoderm taxa. The bottom
827 row represents the effects of perturbation of critical ectodermal regulatory genes. (C) Mechanisms
828 of polarization of NSM in echinoderms. Mesodermal segregation is represented in three
829 echinoderm taxa: Asteroids, Cidaroids, and Euechinoids. In both cidaroids and euehinoids, Nodal
830 signaling via the transcription factor Not segregates oral-aboral NSM cell types by restricting
831 regulatory factors to the aboral side of the embryo. Whereas asteroids show no indication of NSM
832 oral-aboral polarity, cidaroids and euechinoids lineages have undergone dramatic heterochronic
833 shifts since the divergence of these two clades, resulting in the diversification of NSM regulatory
834 states.
835

Fig 1

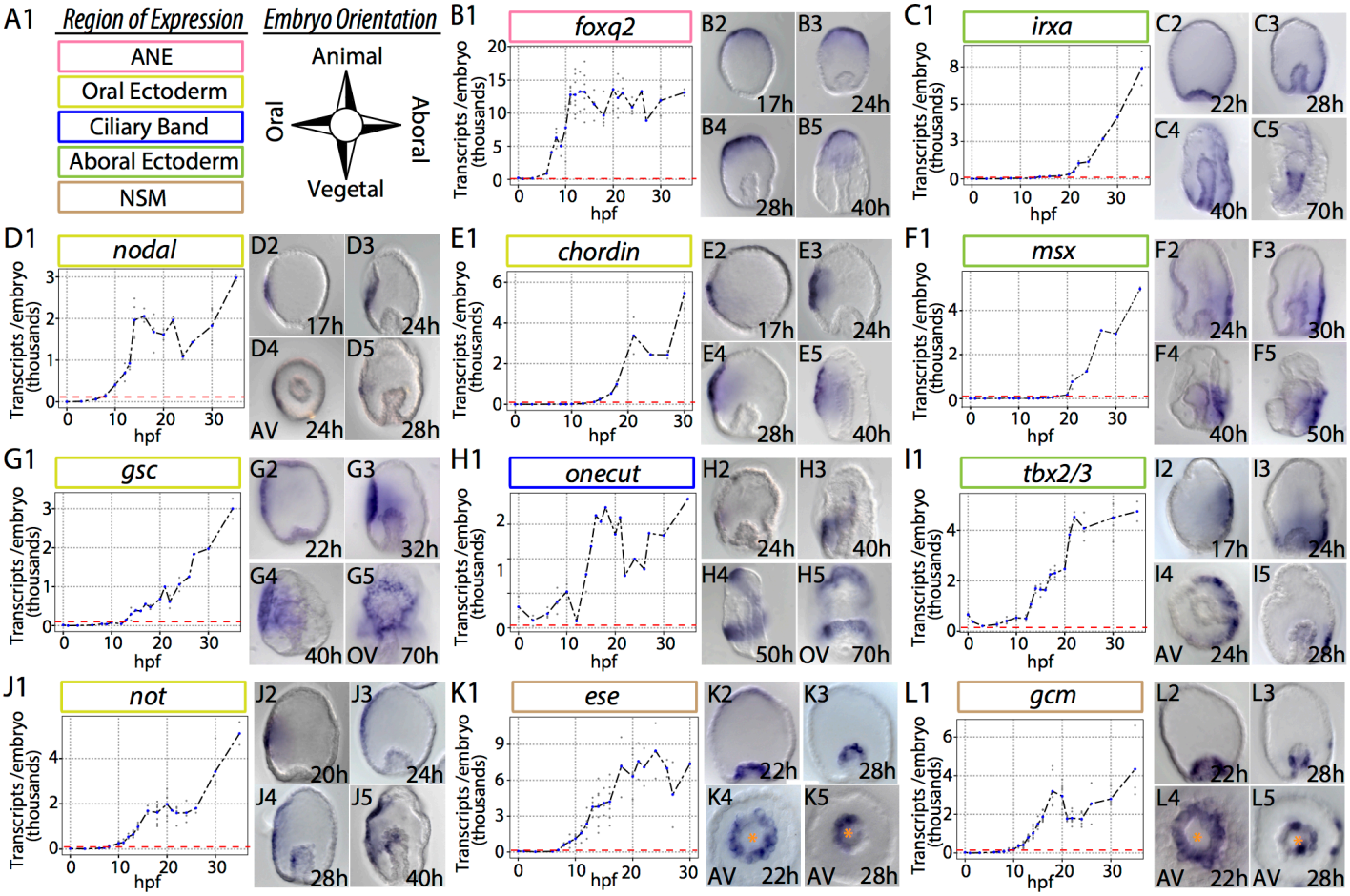
A1
Region of Expression
ANE
Oral Ectoderm
Ciliary Band
Aboral Ectoderm
NSM
Embryo Orientation
Animal
Oral
Aboral
Vegetal
B1
foxq2
B2
B3
B4
B5
17h
24h
28h
40h
C1
irxa
C2
C3
C4
C5
22h
28h
40h
70h
D1
nodal
D2
D3
D4
D5
17h
24h
AV 24h
28h
E1
chordin
E2
E3
E4
E5
17h
24h
28h
40h
F1
msx
F2
F3
F4
F5
24h
30h
40h
50h
G1
gsc
G2
G3
G4
G5
22h
32h
40h
OV 70h
H1
onecut
H2
H3
H4
H5
24h
40h
50h
OV 70h
I1
tbx2/3
I2
I3
I4
I5
17h
24h
AV 24h
28h
J1
not
J2
J3
J4
J5
20h
24h
28h
40h
K1
ese
K2
K3
K4
K5
22h
28h
AV 22h
AV 28h
L1
gcm
L2
L3
L4
L5
22h
28h
AV 22h
AV 28h
Transcripts /embryo (thousands)
hpf

839 **Fig 2**

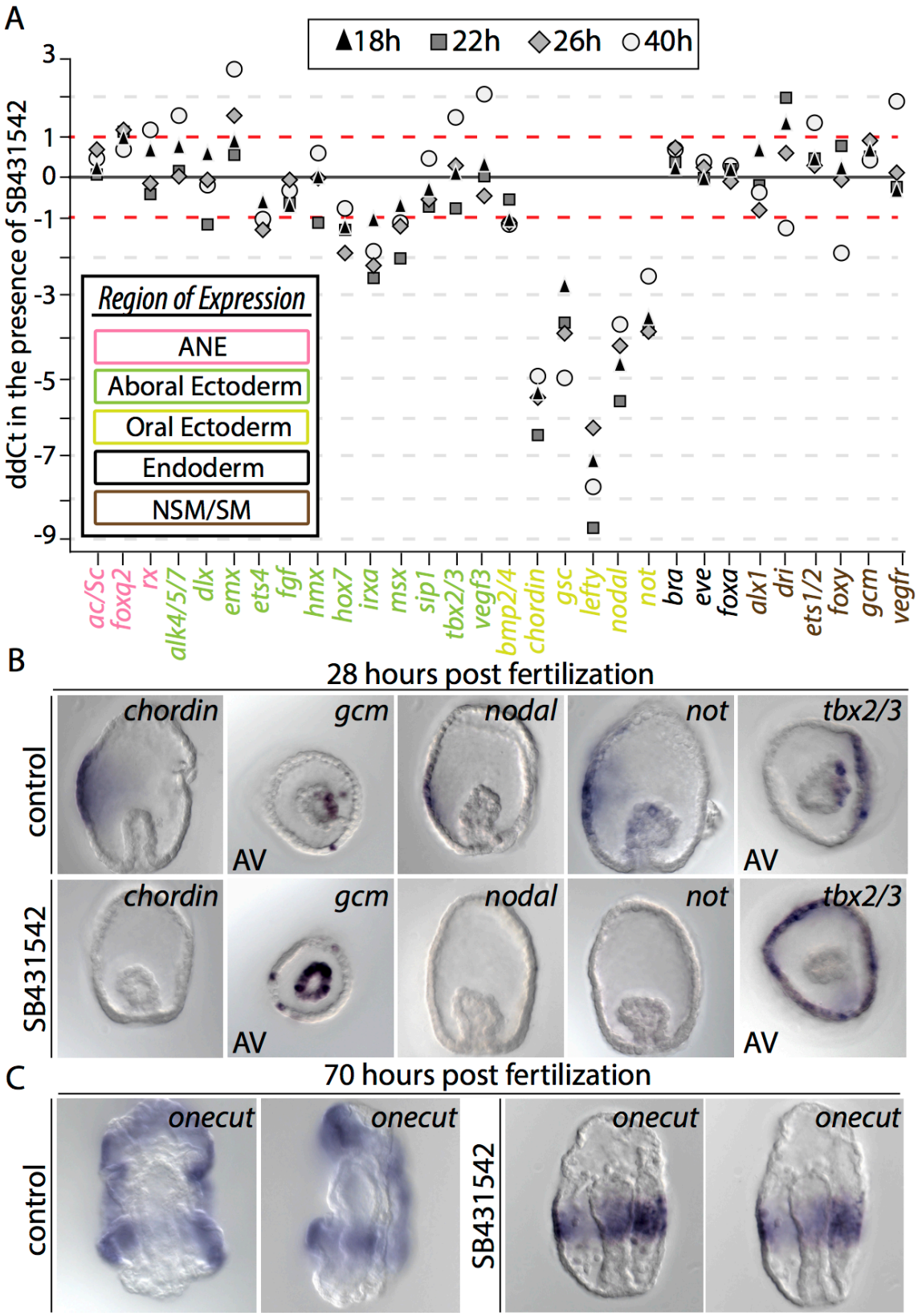
A
18h
22h
26h
40h
ddCt in the presence of SB431542
3
1
0
-1
-3
-5
-7
-9
Region of Expression
ANE
Aboral Ectoderm
Oral Ectoderm
Endoderm
NSM/SM
ac/Sc
foxq2
rx
alk4/5/7
dlx
emx
ets4
fgf
hmx
hox7
irxa
msx
sip1
tbx2/3
vegf3
bmp2/4
chordin
gsc
lefty
nodal
not
bra
eve
foxa
alx1
dri
ets1/2
foxy
gcm
vegfr
B
28 hours post fertilization
control
SB431542
chordin
gcm
nodal
not
tbx2/3
AV
C
70 hours post fertilization
control
SB431542
onecut

840

841 **Fig 3**

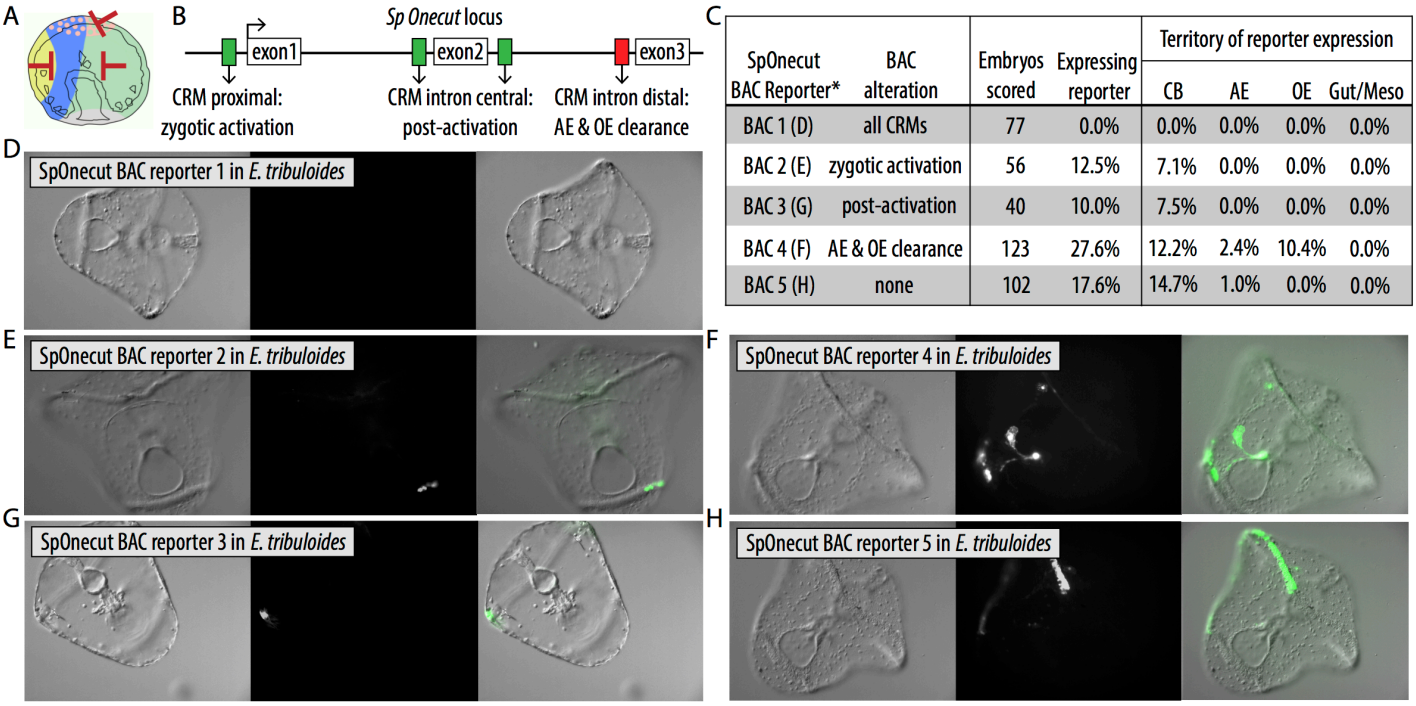

SpOnecut BAC Reporter*	BAC alteration	Embryos scored	Expressing reporter	Territory of reporter expression			
				CB	AE	OE	Gut/Meso
BAC 1 (D)	all CRMs	77	0.0%	0.0%	0.0%	0.0%	0.0%
BAC 2 (E)	zygotic activation	56	12.5%	7.1%	0.0%	0.0%	0.0%
BAC 3 (G)	post-activation	40	10.0%	7.5%	0.0%	0.0%	0.0%
BAC 4 (F)	AE & OE clearance	123	27.6%	12.2%	2.4%	10.4%	0.0%
BAC 5 (H)	none	102	17.6%	14.7%	1.0%	0.0%	0.0%

842

843

Fig 4

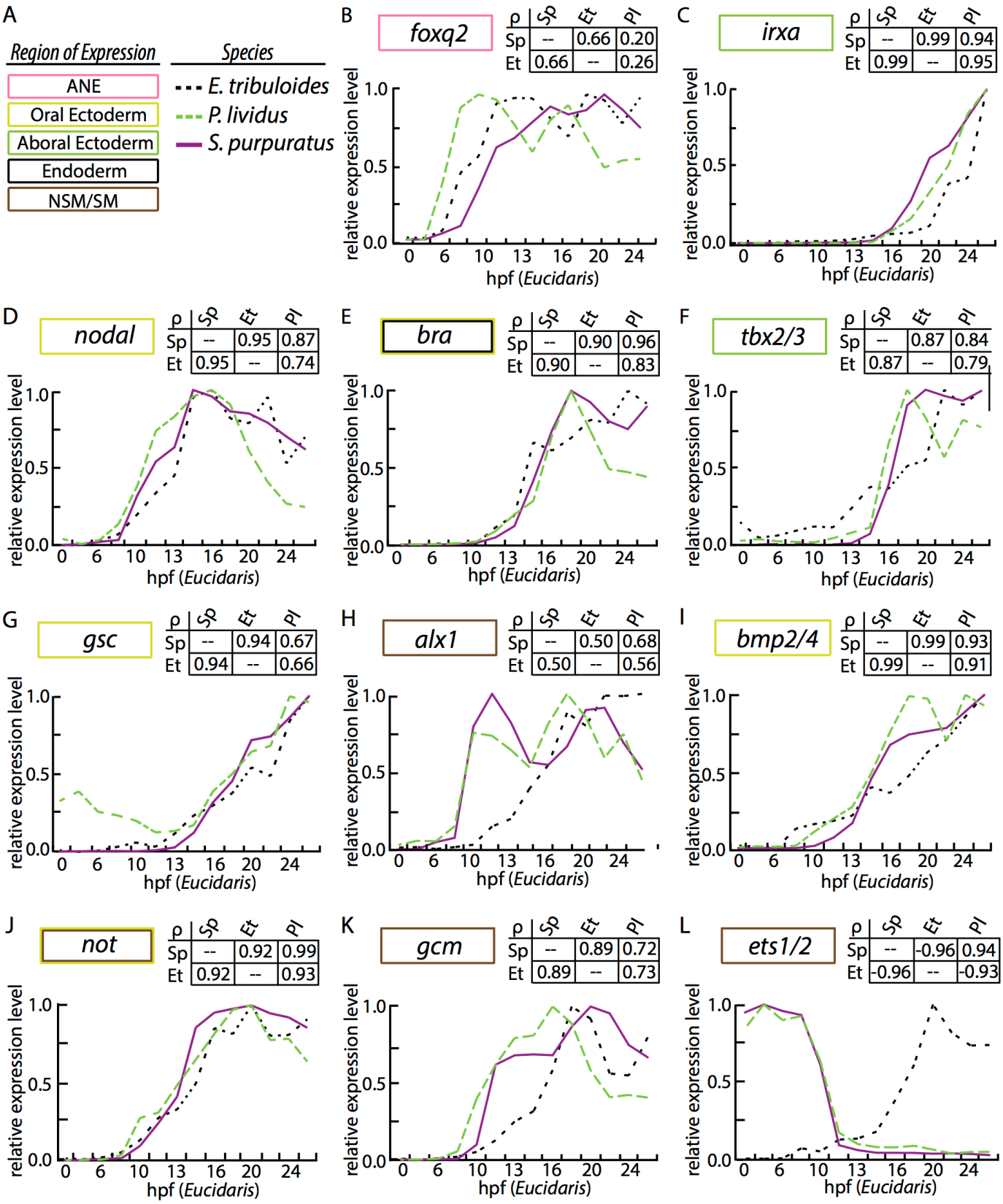
A
Region of Expression
ANE
Oral Ectoderm
Aboral Ectoderm
Endoderm
NSM/SM
Species
E. tribuloides
P. lividus
S. purpuratus
B
foxq2
ρ Sp Et Pl
Sp -- 0.66 0.20
Et 0.66 -- 0.26
C
irxa
ρ Sp Et Pl
Sp -- 0.99 0.94
Et 0.99 -- 0.95
D
nodal
ρ Sp Et Pl
Sp -- 0.95 0.87
Et 0.95 -- 0.74
E
bra
ρ Sp Et Pl
Sp -- 0.90 0.96
Et 0.90 -- 0.83
F
tbx2/3
ρ Sp Et Pl
Sp -- 0.87 0.84
Et 0.87 -- 0.79
G
gsc
ρ Sp Et Pl
Sp -- 0.94 0.67
Et 0.94 -- 0.66
H
alx1
ρ Sp Et Pl
Sp -- 0.50 0.68
Et 0.50 -- 0.56
I
bmp2/4
ρ Sp Et Pl
Sp -- 0.99 0.93
Et 0.99 -- 0.91
J
not
ρ Sp Et Pl
Sp -- 0.92 0.99
Et 0.92 -- 0.93
K
gcm
ρ Sp Et Pl
Sp -- 0.89 0.72
Et 0.89 -- 0.73
L
ets1/2
ρ Sp Et Pl
Sp -- -0.96 0.94
Et -0.96 -- -0.93
relative expression level
1.0
0.5
0.0
0 6 10 13 16 20 24
hpf (Eucidaris)

Fig 5

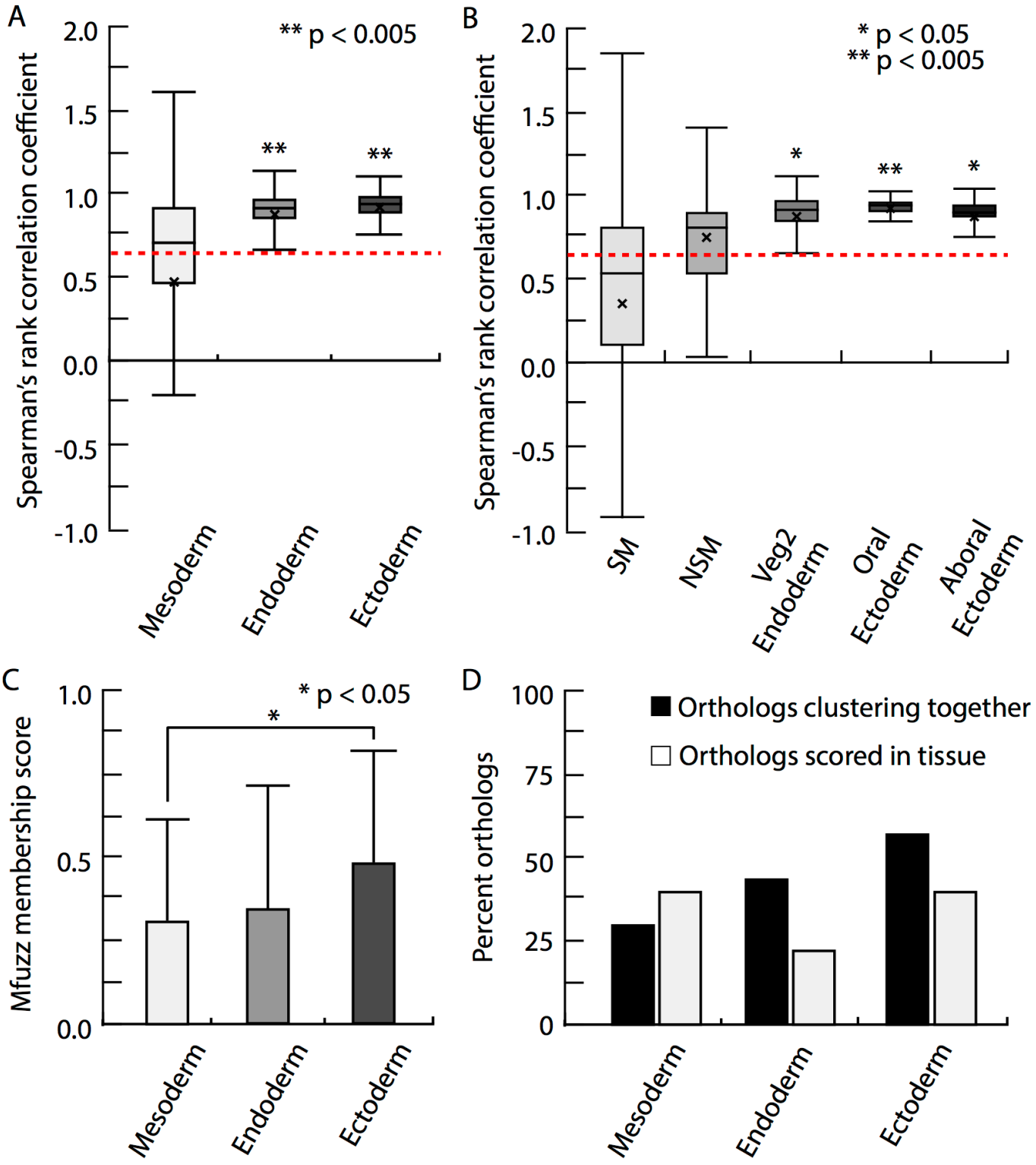
A
** p < 0.005
Spearman's rank correlation coefficient
2.0
1.5
1.0
0.5
0.0
-0.5
-1.0
**
**
Mesoderm
Endoderm
Ectoderm
B
* p < 0.05
** p < 0.005
Spearman's rank correlation coefficient
*
**
*
SM
NSM
Veg2 Endoderm
Oral Ectoderm
Aboral Ectoderm
C
* p < 0.05
Mfuzz membership score
1.0
0.5
0.0
*
Mesoderm
Endoderm
Ectoderm
D
Orthologs clustering together
Orthologs scored in tissue
Percent orthologs
100
75
50
25
0
Mesoderm
Endoderm
Ectoderm

850 **Fig 6**

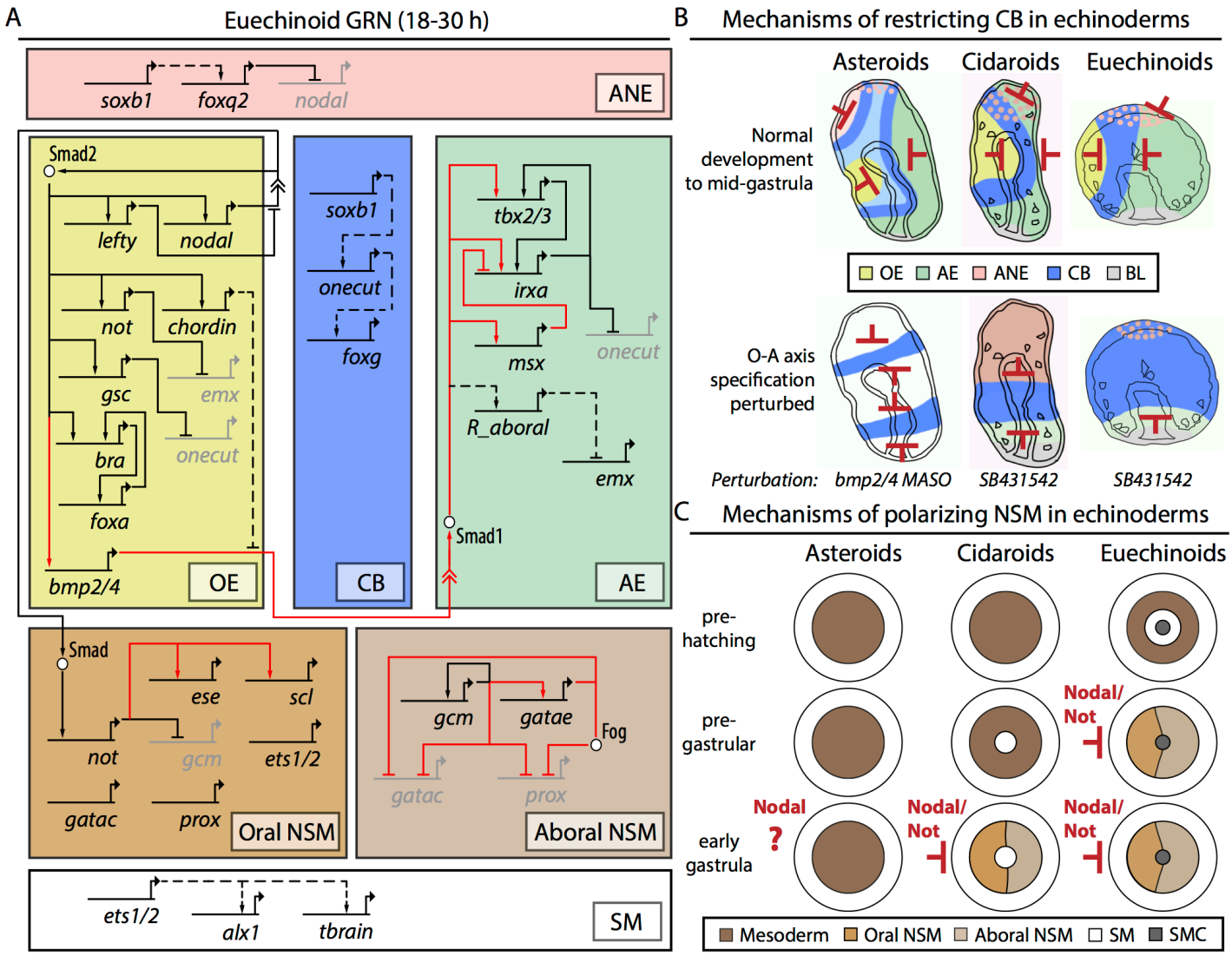

851

852